P11B.10 RAIN AND WET HAIL SPECIFIC ATTENUATION ESTIMATION FOR A 3D SUPERCELL CASE USING RAMS MODEL TO SIMULATE CASA X-BAND AND WSR-88D S-BAND RADAR SIGNALS

L.V. Leon*, G.J. Huang, Y.X. Liu, V.N. Bringi, A. Loftus
Colorado State University, Fort Collins, Colorado, USA

1. INTRODUCTION

A number of different algorithms are available for rain attenuation-correction using the differential propagation phase $_{dp}$ (either directly or as a constraint; e.g., Bringi et al 1990; Matrosov et al 2002; Testud et al 2000; Gorgucci et al 1996; Park et al 2005). But when rain is mixed with wet ice (which frequently occurs in convective storms), the $_{dp}$-based methods will be inaccurate because wet ice (hail/graupel) does not have significant contribution on $_{dp}$ whereas it does contribute significantly to the X-band attenuation. While the attenuation due to the rain component of the mixture can be calculated using path integrated attenuation *PIA* due to rain (based on $_{dp}$), the attenuation due to the wet ice component is very difficult to estimate because of the large variability in the size distribution and water coat thickness which gives rise to large family of *k-Z* relations (*k* is the specific attenuation, Z is the intrinsic reflectivity). In the past, the dual-wavelength (S/X-band) radar technique was developed primarily for hail detection but did need attenuation-correction of the X-band signal due to rain and wet ice along the path (e.g., Tuttle and Rinehart 1983).

Here a technique is developed and evaluated using the microphysics outputs from a Regional Atmospheric Modeling System (RAMS) 2-moment scheme supercell simulation described in Meyers et al (1997) to simulate the CASA (Collaborative and Adaptive Sensing of the Atmosphere) X-band and WSR-88D S-band radar signals. The RAMS model has detailed microphysical information including the liquid fraction of hail and graupel (due to melting or wet growth aloft). A dual-frequency/dual-polarized radar emulator is used to simulate RHI or PPI scans from the RAMS gridded outputs. This paper also presents a preliminary technique to separately estimate the X-band specific attenuation due to rain and wet ice along the path of the CASA dual-polarized X-band radar using the WSR-88D NEXRAD S-band as a reference (i.e., un-attenuated) signal. This technique is examined using sample data[R1] provided by the X-POL and S-POL radars operated during the International H20 Project (IHOP) experiment.

2. Background and Methodology

Attenuation due to wet ice is difficult to correct for even with a polarimetric X-band radar. The impact it has on radar parameters such as reflectivity can be very high in deep convection. Here we treat the wet ice (e.g., hail) as isotropic while the raindrops form a highly oriented medium. To quantify attenuation due to this wet ice along with its vertical extent above the freezing level (separately from the rain attenuation) can help to understand the microphysical processes involved within rapidly evolving convective storms. Methods to correct for rain attenuation make use of the close relation between the differential propagation phase $_{dp}$ and path attenuation (or PIA) (Bringi and Chandrasekar 2001). This relation is the basis of these correction methods were $_{dp}$ is involved either directly or as a constraint. The use of these methods are known to be successful in rain events, but when some wet ice is present, this method is no longer useful because the differential propagation phase is not affected by the isotropic wet ice. This led us to develop[R2] techniques for estimating the attenuation due to rain and wet-ice separately. In Liu et al (2006), a technique was proposed to correct for both rain and wet-ice and separately calculate the attenuation due to each component. . A RAMS model supercell simulation using the one moment scheme, described by Huang et al (2005), was used to simulate X-band and S-band dual-polarized radar RHI scans. Here, a RAMS model supercell simulation using 2 moment scheme (as described by Meyers et al (1997)) is used to simulate dual-polarized X-band and WSR-88D mono-polarized radar data.

To correct the X-band attenuation for rain, the simple attenuation correction method is used (Bringi and Chandrasekar 2001), where for an inhomogeneous path,

$$Z_h^{attenuated} = Z_h^{unattenuated} - 2\int_0^r A_h(s)ds \qquad (1)$$

Knowing that the specific attenuation $A_h=\alpha K_{dp}(r)$ and $K_{dp}=[\ _{dp}(r_2)-\ _{dp}(r_1)]/2(r_2-r_1)$ equation 1 can be re-written as,

$$Z_h^{attenuated} = Z_h^{unattenuated} - \alpha[\Phi_{dp}(r) - \Phi_{dp}(0)] \qquad (2)$$

Since we know that this method will correct only for rain, we can calculate the path integrated attenuation (PIA) as well as A_h as a function of range along the path. To make the correction due to wet-ice at X-band, a non-attenuating wavelength (e.g., S-band) radar reference signal is necessary (but not necessarily the entire range

* *Corresponding author address:* Leyda León, Colorado State University, ECE Dept., Fort Collins, CO 80523-1373 email: leydaleo@engr.colostate.edu

profile). The S-band radar need only provide the (un-attenuated) reflectivity value at the end of the X-band beam. This is used as reference to calculate dual wavelength ratio (DWR) at the end of the path (from now on ΔZ). Note that ΔZ is now the difference between the un-attenuated S-band reflectivity and the rain-corrected X-band reflectivity at the end of the beam. In practice, the S-band and X-band radars will not be collocated and some space/time interpolation will be needed. The TRMM Surface Reflection Technique (SRT) α-adjustment method (Iguchi et al 2000) is used to apportion the ΔZ backwards along the beam. The SRT uses an initial $A_h = \alpha Z^{\beta}$ power law for rain and

it adjusts the coefficient α (assuming fixed β). Here the coefficient β is fixed at 0.6 as in Tuttle and Rinehart (1983). This value may vary depending on the wet-ice mean size. The β exponent was fixed to 0.6 considering that their values (from Tuttle and Rinehart 1983) varied from 0.456 and 0.648 (above and below melting layer, respectively). The starting value of α was set to 0.00048 as in their paper. This α is adjusted such that $\alpha_{adj}=\alpha\varepsilon$, where ε is the attenuation correction factor defined by Iguchi et al. (2000):

$$\varepsilon = \frac{1-10^{\beta\Delta Z/10}}{0.2\ln(10)\beta\int_0^{r_s}\alpha(s)Z_m^{\beta}(s)ds} \qquad (3)$$

and Z_m is the measured X-band reflectivity in units of mm^6 m^-3 (in our case the one that was already corrected for rain attenuation using equation 2). With this defined correction factor, the corrected reflectivity at X-band due to wet ice only can be calculated by,

$$Z_h^{corrected} = \frac{Z_m(r)}{[1-0.2\ln(10)\varepsilon\beta\int_0^{r}\alpha(s)Z_m^{\beta}(s)ds]^{1/\beta}} \qquad (4)$$

3. Datasets

Two different data sets are used in this analysis. The first one is a RAMS supercell case and the second one is an event with rain mixed with wet ice, collected by the X-POL and S-POL radars on June 16, 2002.

Supercell Simulations

A supercell is simulated using the RAMS 2-moment microphysical parameterization described in Meyers et al (1997). It predicts number [R3]concentrations N_t and mixing ratios r of different species like rain, hail and graupel. The gamma distribution is used with shape parameter ν equal to 2. The temperature along with the predicted N_t and r are provided at each grid point. These predicted values are used in a radar emulator that uses a T-matrix scattering code at each grid point along with assumptions on particle shapes, orientations and dielectric constants.

For the rain case, the assumed intercept parameter N_o is fixed to the Marshall-Palmer value of 8000 $mm^{-1}m^{-3}$. The raindrops are assumed to be oblate with the equilibrium axis ratios given by Beard and Chuang shape model. Also the canting angle is assumed to be Gaussian in shape with standard deviation of 5°. For the hail/graupel case, it is assumed that they are oblate in shape with axis ratio of 0.8 with random orientation. The distinction of dry and wet ice is done by using the liquid fraction given by the RAMS model. Polarimetric radar variables at X-band are calculated such as reflectivity (Z_h), specific differential phase (K_{dp}) and also the specific total attenuation (A_h) as well as the attenuation contributions from each particle type (A_h^{rain}, $A_h^{dry\text{-}ice}$, $A_h^{wet\text{-}ice}$, $A_h^{graupel}$). For the S-band case, only the reflectivity (Z_h) profiles are used here. . With these gridded data, RHI and PPI scans were simulated for both frequencies.

X-POL/S-POL dataset from IHOP

The X-POL/S-POL datasets include PPI scans at different elevation angles (0.5 to 10.5º). This provides X-band dual-polarized radar data as well as S-band reflectivity data (note, even though S-POL radar is dual-polarized, no polarimetric variable is used other than the reflectivity). These radar data were analyzed in the same way as the supercell simulation dataset.

4. Results

Supercell Simulations

Using the radar emulator results from the RAMS model supercell simulation, variables like reflectivity, specific attenuation and specific differential phase were computed.[R4] Fig. 1 shows gridded data of intrinsic reflectivity along with contours of specific attenuation of rain and wet ice.

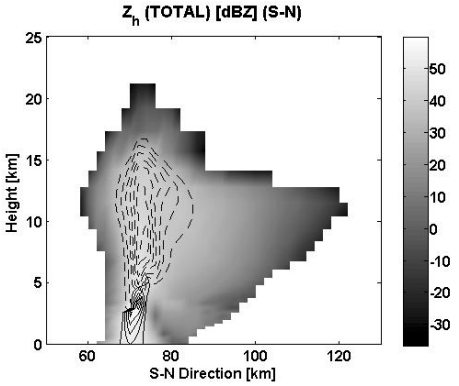

Fig. 1: True specific attenuation contours of rain (solid line) and hail (dashed line) over true X-band reflectivity (background)[R5] on the S-N Direction cross-section (RHI scan) using RAMS model.

The path integrated attenuation *PIA* was calculated by integrating the specific attenuation A_h provided by the RAMS model microphysics. . The results are shown in Fig. 2, where the total *PIA* (rain + wet ice), the *PIA* due

to rain, and the *PIA* due to wet ice increase up to 45, 18 and 25 dB, respectively. These values are derived from the true specific attenuation. Also shown is the dual-wavelength ratio, i.e., $Z_h(S)$-$Z_h(X)$ with Gaussian measurement noise added (σ=1dB at each frequency). Note that $Z_h(X)$ is attenuated by all hydrometeors along the path. In the same way, Gaussian noise with σ=2° was added to the specific differential phase K_{dp} that was used to retrieve the differential phase $_{dp}$ at X-band.[R6]

This $_{dp}$ was used to correct for rain using the simple attenuation correction method in equation 2. Fig. 3 shows a typical correction for a radar beam at 2° elevation angle that just contains rain. As can be seen, the simple attenuation correction method worked well for rain only and compares well with the S-band Z.

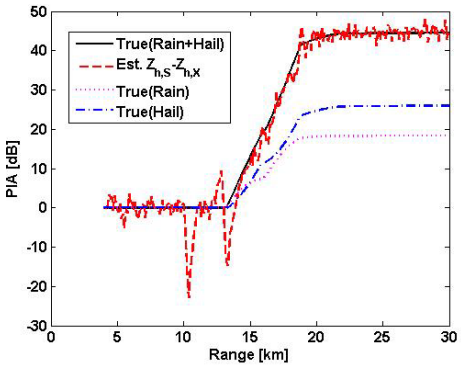

Fig. 2: Path integrated attenuations (PIA) at 12.6° in elevation for total (rain + wet ice), rain and wet ice.

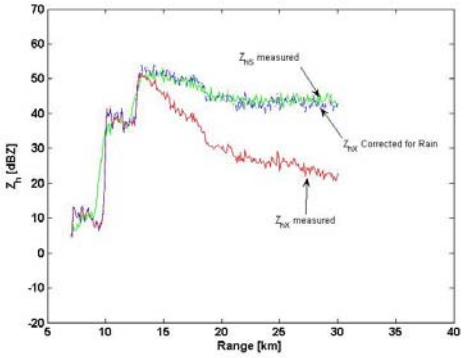

Fig. 3: Rain attenuation correction of the X-band signal using RAMS model data. This radar beam is at 2° in elevation.

On the other hand, when this method is applied to a radar beam containing rain mixed with wet ice, this correction method based on $_{dp}$ is not enough (see Fig. 4). As expected from the *PIA* calculations, the rain attenuation is about the 18 dB. This is the amount corrected by the simple attenuation correction method. We can observe that the signal is still attenuated because of the wet ice component thus affecting the signal up to 25 dB. To correct for this additional attenuation, the α-adjustment method was used where the S-band (un-attenuated) Z at the end of the beam is used as reference to get the ΔZ = 28.9 dB in this case. This way the X-band Z profile that was just corrected for rain is retrieved using the variant of the SRT method described earlier in equation 4. . Fig. 4 shows the X-band Z corrected for both rain and wet ice compared to the un-attenuated S-band Z. Comparing the intrinsic PIA due to wet ice in Fig. 2 (25 dB at the end of the beam) with ΔZ in Fig. 4 (28.9 dB) we can note the consistency between them to within several dB. Notice that if we compare the S-band Z and the X-band corrected one in Fig. 4; they are within a few dB along the entire beam.

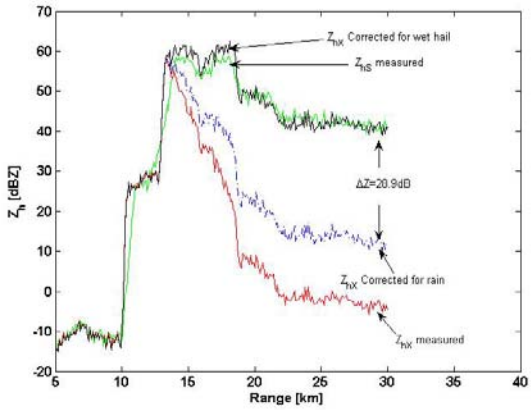

Fig. 4: Rain and wet-ice attenuation correction of the X-band signal using RAMS model data. Radar beam at 12.6° in elevation.

The retrieval procedure for obtaining the vertical structure of the specific attenuation is based on the simulated RHI scan beams. Contours of the specific attenuation due to rain are shown in Fig. 5 and that due to wet ice is shown in Fig. 6. These vertical sections are from the core of the storm where the maximum Z[R7] is. In each figure the left panel shows the intrinsic specific attenuation from RAMS microphysical outputs while the right panels show the simulated radar-based retrievals.

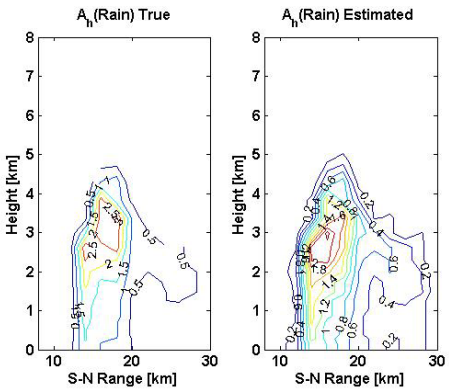

Fig. 5: Rain attenuation vertical cross-section retrieval for the S-N direction for an RHI scan. [R8]

In Fig. 5, the peak attenuation due to rain is well estimated with 0.39 dB/km maximum RMS error from

the intrinsic values. The same 0.20 dB/km maximum RMS error from its intrinsic values was found in the wet ice case.

X-POL/S-POL dataset from IHOP

The XPOL radar is described in Anagnostou et al. (2004). The SPOL radar was operated by NCAR. These two radars were in close proximity to each other. The beams from the two radars were 'matched' by Dr. Marios Anagnostou and provide to us. The same procedure for estimating the specific attenuation at X-band for rain and wet ice was followed using the X-POL/S-POL radar data. Fig. 7 shows a range profile at 2º elevation angle depicting the X-band Z correction for both rain and wet ice. In this profile the ΔZ=9 dB at the end of the beam. It is shown that the correction is good if we compare the attenuation-corrected X-band Z with the un-attenuated S-band Z in spite of the beams not being exactly matched in range resolution and sampling time.

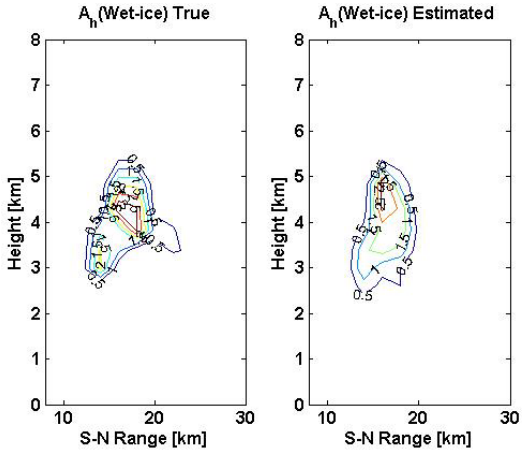

Fig. 6: Hail attenuation cross-section retrieval for the S-N direction for an RHI scan.

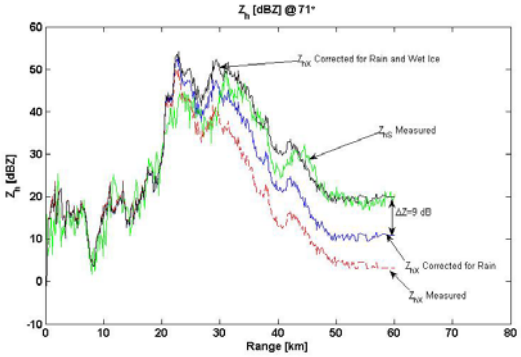

Fig. 7: Rain and wet-ice attenuation correction of the X-band signal using X-POL and S-POL data. A PPI scan at 2° in azimuth and 71° in elevation was used.

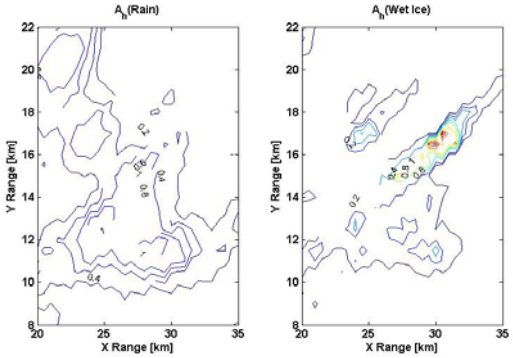

Fig. 8: Rain (left panel) and Wet-ice (right panel) attenuation retrieval using X-POL and S-POL data.

Fig. 8 shows the contours of the specific attenuation for rain (left panel) and wet ice (right panel). These are estimated from the XPOL/SPOL from the PPI scan data set at 2º elevation angle. The results look 'reasonable' when overlaid with the Z contours (not shown here).

5. Conclusions

RAMS model supercell simulation data and actual X-POL/S-POL radar data were used to analyze the proposed technique for separating the attenuation due to rain and wet ice when the beam path contains a mixture of both species. For both datasets the X-band Z correction showed good agreement when compared to the S-band un-attenuated signal as shown in Figs. 4 and 7.The rain attenuation was estimated using the X-band $_{dp}$ (e.g. Bringi and Chandrasekar 2001). [R9]The wet ice attenuation was based on the SRT-like algorithm where only the ΔZ between S-band Z and X-band Z at the end of the beam was used (Iguchi et al. 2000). Fig. 5 and Fig. 6 showed that radar simulations were comparable to the intrinsic values for the RAMS microphysics. It showed that having a dual-polarized X-band radar provides to correct for rain attenuation while having the reflectivity of an un-attenuated signal such as the S-band at the end of the beam, can provide a way to successfully correct for wet ice attenuation at X-band.

Single wavelength X-band radars are affected by attenuation. It is intended to analyze real data obtained from the Collaborative and Adaptive Sensing of the Atmosphere (CASA) radars using the WSR-88D as a reference signal as a future work.

Acknowledgements: This work was supported by the Engineering Research Center program of the NSF under award number 0313747. The authors are grateful to Dr Marios Anagnostou and Prof. Emmanouil Anagnostou of the University of Connecticut for providing us the matched XPOL/SPOL datasets.

REFERENCES

Anagnostou, E. N., Anagnostou, M. N., Krajewski, W. F., Kruger, A., Miriovsky, B. J., 2004: High-Resolution Rainfall Estimation from X-Band Polarimetric Radar Measurements, *J. of Hydromet.*, **5**, Issue 1, 110− 128

Bringi, V.N. and V. Chandrasekar, 2001: Polarimetric doppler weather radar: principles and applications. Cambridge.

Bringi, V.N., V. Chandrasekar, N. Balakrishnan, and D.S. Zrni , 1990: An examination of propagation effects in rainfall on radar measurements at microwave frequencies. *J. Atmos. Oceanic Technol.*, 7, 829-840.

Bringi, V.N. and A. Hendry, 1990: Technology of polarization diversity radars for meteorology. In *Radar in Meteorology*. D. Atlas, Ed., 153-190, Boston, MA, American Meteorological Society.

Gorgucci, E., G. Scarchilli, and V. Chandrasekar, 1996: Error structure of radar rainfall measurement at C-band frequencies with dual-polarization algorithm for attenuation correction. *J. Geophys. Res.*, **101**, 26461-26471.

Huang, G.J., V.N. Bringi, S. van den Heever, and W. Cotton, 2005: Polarimetric radar signatures from RAMS microphysics. *AMS Conference on Radar Meteorology*, 24-29.

Iguchi, T., T. Kozu, R. Meneghini, J. Awaka, and K. Okamoto, 2000: Rain-Profiling Algorithm for the TRMM Precipitation Radar. *J. Appl. Meteo.,* **39**, 2038-2052.

Liu,Y., , G.J. Huang, V.N. Bringi and S. van den Heever, 2006: Estimation of X-band radar attenuation due to wet hail: A simulation study using RAMS supercell case and dual-wavelength (S/X-band) radar. *ERAD06*, 49-52.

Matrosov, S.Y., K.A. Clark, B.E. Martner, and A. Tokay, 2002: X-band polarimetric radar measurements of rainfall. *J. Appl. Meteor.*, **41**, 941-952.

Meyers, M. P., R. L. Walko, J. Y. Harrington, W. R. Cotton, 1997: New RAMS cloud microphysics parameterization. Part II: The two-moment scheme. *Atmos. Res.*, **45**, 3-39.

Park, S.G., V.N. Bringi, V. Chandrasekar, M. Maki and K. Iwanami, 2005: Correction of radar reflectivity and differential reflectivity for rain attenuation at X band. Part I: theorectical and empirical basis. *J. Atmos. Oceanic Technol.*, **22**, 1621-1632.

Park, S.G., M. Maki, K. Iwanami, V.N. Bringi and V. Chandrasekar, 2005: Correction of radar reflectivity and differential reflectivity for rain attenuation at X band. Part II: evaluation and application. *J. Atmos. Oceanic Technol.*, **22**, 1633-1655.

Tuttle, J.D. and R.E. Rinehart, 1983: Attenuation correction in dual-wavelength analyses. *J. Climate Appl. Meteor.*, **22**, 1914-1921.

Testud, J., E.L. Bouar, E. Obligis, and M. Ali-Mehenni, 2000: The rain profiling algorithm applied to polarimetric weather radar. *J. Atmos. Oceanic Technol.*, **17**, 322-356.